Oncogene (2020) 39:1498–1513
https://doi.org/10.1038/s41388-019-1081-2

ARTICLE

Histone deacetylases, Mbd3/NuRD, and Tet2 hydroxylase are crucial regulators of epithelial–mesenchymal plasticity and tumor metastasis

Ayse Nihan Kilinc[1,2] · Nami Sugiyama[1] · Ravi Kiran Reddy Kalathur[1] · Helena Antoniadis[1] · Huseyin Birogul[1] · Dana Ishay-Ronen[1] · Jason T. George[3,4] · Herbert Levine[3,5] · Mohit Kumar Jolly[6] · Gerhard Christofori[1]

Received: 11 March 2019 / Revised: 16 October 2019 / Accepted: 17 October 2019 / Published online: 30 October 2019

Abstract

An epithelial–mesenchymal transition (EMT) represents a basic morphogenetic process of high cell plasticity underlying embryogenesis, wound healing, cancer metastasis and drug resistance. It involves a profound transcriptional and epigenetic reprogramming of cells. A critical role of epigenetic modifiers and their specific chromatin modifications has been demonstrated during EMT. However, it has remained elusive whether epigenetic control differs between the dynamic cell state transitions of reversible EMT and the fixed differentiation status of irreversible EMT. We have employed varying EMT models of murine breast cancer cells to identify the key players establishing epithelial–mesenchymal cell plasticity during reversible and irreversible EMT. We demonstrate that the Mbd3/NuRD complex and the activities of histone deacetylases (HDACs), and Tet2 hydroxylase play a critical role in keeping cancer cells in a highly metastatic mesenchymal state. Combinatorial interference with their functions leads to mesenchymal–epithelial transition (MET) and efficiently represses metastasis formation by invasive murine and human breast cancer cells in vivo.

Introduction

Epithelial–mesenchymal transition (EMT) is a critical morphogenetic process during embryonic development and wound healing [1–4]. The dynamic transitions from an epithelial to a mesenchymal cell state have also been shown to promote cancer cell stemness and tumorigenicity, cancer cell invasion, metastatic dissemination, and drug resistance [2, 4–6]. The profound changes in gene expression and the high cell plasticity accompanying the dynamic process of EMT and its reversion, mesenchymal–epithelial transition (MET), imply a key role of the rearrangement of chromatin states by epigenetic modifications [7, 8]. While the importance of epigenetic modifications and the respective chromatin-modifying enzymes has been documented [7, 8], the actual contribution of epigenetic changes to epithelial–mesenchymal cell plasticity, notably to the reversibility or irreversibility of EMT, is poorly understood.

Histone deacetylases (HDACs) catalyze the removal of acetyl groups from lysine residues of histones, leading to chromatin condensation and repression of gene expression [9]. The inhibition of HDAC activity has been implicated in the conversion of mesenchymal cells into an epithelial state in breast, ovarian, bladder, and pancreatic cancer cells [10–12]. HDACs, in particular HDAC1 and HDAC2, predominantly function as components of stable multi-protein complexes, including CoREST, Sin3a, and NuRD, and thereby are recruited to specific target genes [13–15]. For example, lysine-specific demethylase 1 (Lsd1) forms a

Supplementary information The online version of this article (https://doi.org/10.1038/s41388-019-1081-2) contains supplementary material, which is available to authorized users.

✉ Gerhard Christofori
gerhard.christofori@unibas.ch

[1] Department of Biomedicine, University of Basel, 4058 Basel, Switzerland

[2] Department of Chemical & Biological Engineering, Princeton University, 303 Hoyt Laboratory, William Street, Princeton, NJ 08544, USA

[3] Center for Theoretical Biological Physics, Rice University, Houston, TX, USA

[4] Medical Science Training Program, Baylor College of Medicine, Houston, TX, USA

[5] Departments of Bioengineering and Physics, Northeastern University, Boston, MA 02115, USA

[6] Centre for BioSystems Science and Engineering, Indian Institute of Science, Bangalore 560012, India

complex with Sin3a to maintain the epithelial state and thereby to inhibit breast cancer invasiveness and stemness [16]. Lsd1 also exerts its metastasis inhibition function by acting as an integral component of the Mi-2/nucleosome remodeling and deacetylase (NuRD) complex in breast cancer [17]. In the context of an EMT, the transcription factor Snail represses the E-cadherin (Cdh1) gene by forming complexes with Sin3a [18] and NuRD complexes [19]. The HDAC1/2-containing NuRD complex is also bound by master regulators of EMT, such as Twist and Zeb2, and directed to the promoter region of the E-cadherin (*Cdh1*) gene to silence its expression [20, 21].

NuRD complexes can be formed by various combinations of different subunits to provide functional specificity, an example being the HDAC1 and HDAC2-containing Methyl-CpG-binding domain 3 (Mbd3)/NuRD complex [22]. Mbd3 is a non-enzymatic component of the Mbd3/NuRD complex with critical functions in lineage commitment of embryonic stem (ES) cells [23, 24]. Underscoring its crucial function in regulating cell plasticity, the Mbd3/NuRD complex serves as a molecular block, and the depletion of Mbd3 allows a more efficient conversion of mouse embryonic fibroblasts (MEFs) into induced pluripotent stem (iPS) cells [25].

Mammalian Mbd3 is the only Mbd family protein that is not able to recognize methylated CpG dinucleotides due to an amino acid change in the Mbd domain [26, 27]. It has been reported that Mbd3 is able to recognize 5-hydroxymethylcytosine (5hmC) sites and recruit Mbd3/NuRD to these sites in mouse ES cells by binding to Tet1 [28], a member of the Tet hydroxylase family. Tet1, 2, and 3 hydroxylases contribute to active DNA demethylation by catalyzing the sequential oxidation of methylated cytosines (5mC) to 5-hydroxymethylcytosine (5hmC), 5-formylcytosine (5fC), 5-carboxylcytosine (5caC), and decarboxylation to unmodified cytosine [29, 30]. However, it has been also suggested that Mbd3-binding to DNA does not depend on 5hmC [31]. On the other hand, Tet hydroxylases have been implicated in the initiation of MET as a prerequisite for MEFs to undergo iPS cell reprogramming [32]. Here, using cellular models of fixed, irreversible EMT and of reversible EMT, we have delineated the central role of HDACs, the Mbd3/NuRD complex and Tet2 hydroxylase in the maintenance of the mesenchymal state of murine breast cancer cells in vitro and primary tumor growth and metastasis in vivo.

Results

Generation of a fixed, irreversible EMT system

We set out to establish in vitro model systems to investigate the dynamic transitions underlying reversible EMT as compared with irreversible EMT. As a model for a reversible EMT we used Py2T murine epithelial mammary carcinoma cells which upon treatment with TGFβ for >10 days underwent a full EMT, while when depleted of TGFβ readily revert to their epithelial state [33]. Contrasting this reversible EMT model, we generated an in vitro irreversible EMT model (adapted from reference [34]). Py2T cells were supplemented with MEGM media (mammary epithelial cell growth media) at different concentrations (0, 0.5, 3, 7%) of fetal bovine serum (FBS) to generate irreversible EMT cells (Supplementary Fig. S1a). Among the concentrations tested, 7% FBS-supplemented MEGM media led to an efficient generation of mesenchymal phenotype cells in the absence of TGFβ (Supplementary Fig. S1a). However, even with an extended period of induction of mesenchymal morphology (up to 20 days) with 7% FBS MEGM media, upon changing to normal growth media (10% FBS in DMEM) the mesenchymal cells reverted to an epithelial state (Supplementary Fig. S1a,b). We therefore extended the duration of culturing Py2T cells in 7%FBS MEGM medium to 3 months, when the cells retained their mesenchymal morphology upon subsequent culture in normal growth media (Fig. 1a). Of these, individual mesenchymal phenotype cells were expanded as cell clones which stably maintained their mesenchymal phenotype (referred to as M clone cells M1, M2, and M3; Fig. 1a, b). In contrast, long-term TGFβ-treated Py2T cells (referred to as Py2T-LT cells) reverted to their epithelial state, when TGFβ was withdrawn from the culture medium (referred to as Py2T-LT MET cells; Fig. 1b).

The M clone cells stably expressed genes associated with a mesenchymal state, including fibronectin (Fn1), vimentin (Vim), N-cadherin (N-cad), Snail, Zeb1, and Twist1, whereas epithelial genes, such as E-cadherin (E-cad), were only found at low levels (Fig. 1c, d). Py2T cells treated with TGFβ (Py2T-LT) also expressed mesenchymal markers, yet upon TGFβ withdrawal the cells regained the expression of E-cad and lost the expression of Fn1, Vim, N-cad, Snail, Zeb1, and Twist1 (Py2T-LT MET cells; Fig. 1c, d). Immunofluorescence analysis revealed that M clone cells maintained their mesenchymal state by expressing Vim and lacking E-cad at the cell membranes, similar to Py2T-LT cells. By contrast, Py2T-LT MET cells lost Vim expression and re-expressed E-cad at the cell membranes (Fig. 1e). These results show that TGFβ-induced Py2T-LT cells revert from a mesenchymal state to an epithelial state upon withdrawal of the EMT inducer TGFβ, while M clone cells sustain their mesenchymal phenotype in basal culture conditions even in the absence of TGFβ.

M clone cells are highly tumorigenic and metastatic

Next, we assessed the tumorigenic potential of Py2T-LT and M clone cells by orthotopic transplantation into the

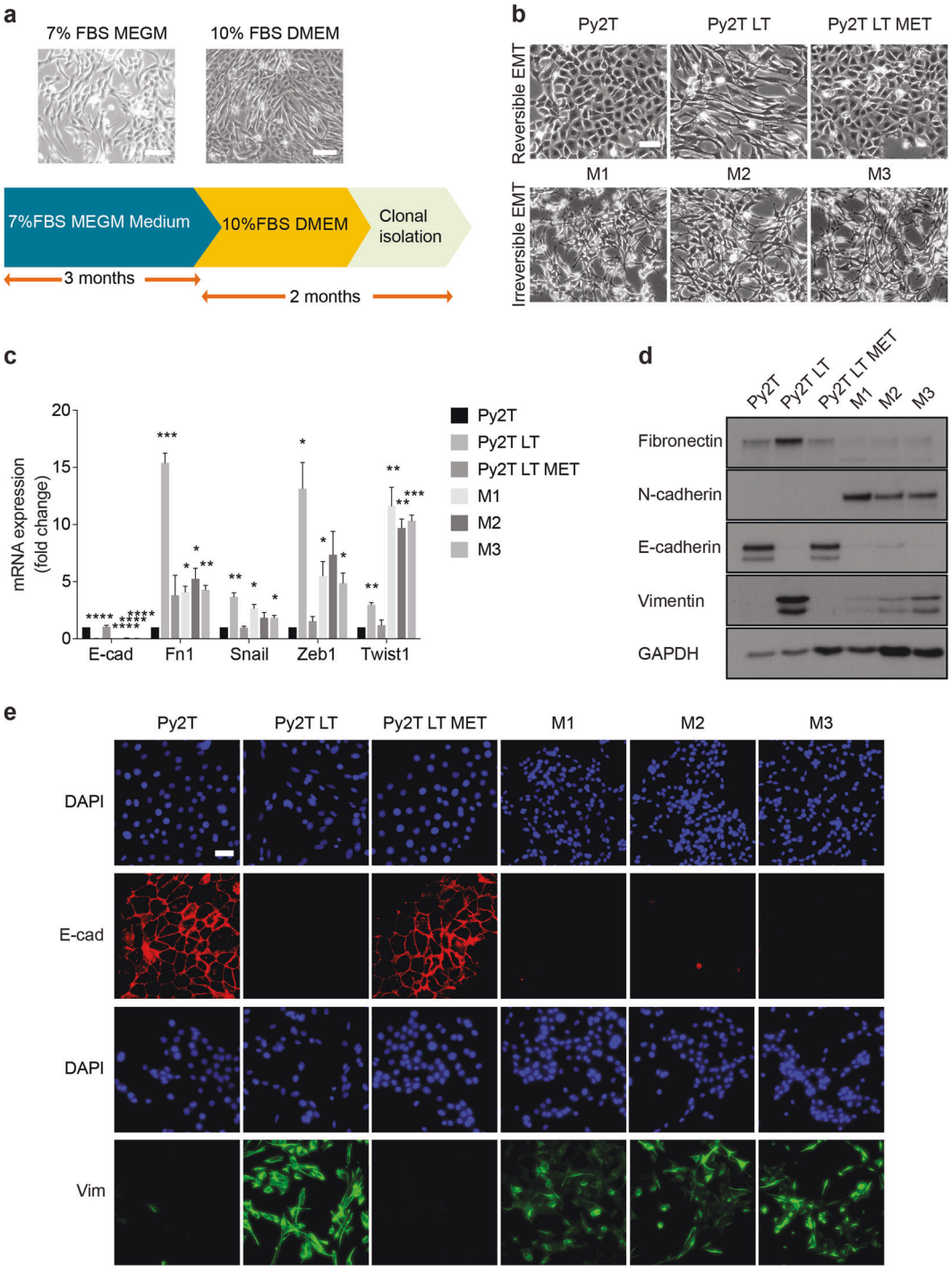

mammary fat pads of immunodeficient NOD/Scid;common γ receptor$^{-/-}$ (NSG) mice. M1 and M3 clone cells showed significantly faster tumor growth than Py2T-LT cells (Fig. 2a). Immunofluorescence analysis revealed low E-cad expression and high Vim expression in tumors of both Py2T-LT and M clone cells (Fig. 2b), indicating that they formed mesenchymal phenotype tumors in vivo, most likely due to the local production of TGFβ by the inflammatory tumor microenvironment [33]. Almost all mice bearing M clone tumors developed macroscopic lung metastases, while only 50% of the mice bearing Py2T-LT tumors showed metastatic lesions (Fig. 2c). Upon tail vein injection of Py2T-LT, M1, and M3 clone cells, all mice developed metastasis, however, the M clone cells initiated a strikingly higher number of metastases and larger metastatic lesions in the lungs as compared with Py2T-LT cells (Fig. 2d–f).

Orthotopic injection of limiting dilutions of cells into immunodeficient BALB/c Rag2$^{-/-}$; common γ receptor$^{-/-}$

◀ **Fig. 1** In vitro characterization of irreversible EMT cells (M clone cells). **a** Scheme of the generation of an irreversible EMT system (M clone cells). Phase-contrast microscopy of Py2T cells cultured in 7% FBS MEGM media for 3 months, subsequently cultured in 10% FBS DMEM for 37 days, respectively. Scale bar, 100 µm. **b** Phase-contrast microscopy of Py2T cells, Py2T cells treated for >20 days with TGFβ (Py2T-LT), Py2T-LT cells upon TGFβ withdrawal (Py2T-LT MET), and M1, M2, and M3 clone cells. Scale bar, 100 µm. **c** Expression of E-cadherin (E-cad), fibronectin (Fn1), Snail, Zeb1, Twist1 was determined by quantitative RT-PCR in Py2T, Py2T-LT, and Py2T-LT MET cells and in M1, M2, and M3 clone cells. Fold changes are related to expression levels in Py2T cells. Data are displayed as mean ± SEM. Statistical values were calculated using a paired, two-tailed *t*-test. $*P < 0.05$; $**P < 0.01$, $***P < 0.001$; $****P < 0.0001$. **d** Expression of fibronectin (Fn1), N-cadherin (N-cad), E-cadherin (E-cad), and Vimentin (Vim) was determined by immunoblotting in Py2T, Py2T-LT, and Py2T-LT MET cells and in M1, M2, and M3 clone cells. Immunoblotting for GAPDH was used as a loading control. **e** Immunofluorescence microscopy analysis of changes in the localization and expression levels of marker proteins in Py2T, Py2T-LT, and Py2T-LT MET cells and M1, M2, and M3 clone cells. Cells were stained with antibodies against the epithelial marker E-cadherin (E-cad) and the mesenchymal marker vimentin (Vim). DAPI was used to visualize nuclei. Scale bar, 50 µm

(RG) mice revealed that M clone cells exhibited a significantly higher tumor-initiating capability than Py2T-LT cells (Fig. 2g) and that all tumors formed by M clone cells could be serially transplanted (Fig. 2h). These data demonstrate a higher ability of irreversible EMT cells to initiate tumors and to colonize the lung as compared with reversible EMT cells.

HDAC inhibition causes a partial MET in M clones

We next assessed whether the maintenance of the mesenchymal state of M clone cells depended on epigenetic regulators and modifications. We screened a number of epigenetic inhibitors for a reversion of M clone cells to an epithelial state, including 3-Deazaneplanocin A (DZNep), a pharmacological inhibitor of the histone methyltransferase Ezh2 [35], a key player in the initiation of an EMT [36], the DNA methylation inhibitor 5-Aza-2′-deoxycytidine (DAC) [37], and the HDAC inhibitor Trichostatin A (TSA) [38]. Among these, only TSA induced morphological changes toward an epithelial state in M clone cells, concomitant with a marked increase in the expression of E-cad, yet no significant change in the expression of Fn1 and N-cad (Supplementary Fig. S2a–d). These results indicated that histone deacetylation played a critical role in maintaining the mesenchymal phenotype of M clone cells. Bisulfite pyrosequencing of the E-cad gene promoter in reversible and irreversible EMT cells did not show any significant change in the extent of methylated CpG islands (Supplementary Fig. S2e), indicating that changes in DNA methylation were not accountable for the difference between a reversible and an irreversible EMT. The more specific inhibitor of Ezh2 methyltransferase activity EPZ005687 [39] also did not elicit any changes in cell morphology or EMT marker expression (Supplementary Fig. S2f, g).

Based on the roles of HDAC Class I inhibitors in the reversion of EMT in pancreatic cancer cells [40] and our results with TSA, we treated Py2T-LT cells and M clone cells with two more HDAC inhibitors, the selective HDAC Class I inhibitor Tacedinaline (CI994) and the non-selective HDAC inhibitor Panobinostat (LBH589) [41]. Consistent with the gain of an epithelial morphology, the efficient inhibition of HDAC activities by CI994 and LBH589 increased E-cad and Claudin4 (Cldn4) protein and mRNA expression in all M clone cells, yet with varying effects in mRNA and protein expression of the mesenchymal markers N-cad, Fn1, Vim, and Zeb1 (Fig. 3a–c; Supplementary Fig. S3a–c). In comparison, despite an efficient inhibition of HDAC activity, Py2T-LT cells showed no obvious alterations in E-cad, Fn1, N-cad, and Vim protein and mRNA expression upon treatment with CI994 or LBH589 (Fig. 3a–c). Also, E-cad was localized to cell membranes in M clone cells treated with CI994 and LBH589, while Vim expression was maintained, and no change was observed in Py2T-LT cells treated with HDAC inhibitors in the presence of TGFβ (Fig. 3d, Supplementary Fig. S3d).

These results indicate that M clone cells can be partially reverted to an epithelial state by HDAC inhibition, while Py2T-LT cells only revert to an epithelial phenotype upon withdrawal of TGFβ.

The Mbd3/NuRD complex is critical for a mesenchymal state

We next assessed how HDACs were involved in the regulation of epithelial–mesenchymal plasticity. It is well established that multimeric protein complexes facilitate HDAC functions [15]. For example, the Mbd3/NuRD complex exerts its activity at least in part via HDACs and plays a critical role in the efficient reprogramming of MEFs into iPS cells [25]. Since a MET has been shown critical during efficient iPS cell reprogramming [42], we tested whether Mbd3 contributed to the fixed mesenchymal state of M clone cells. Indeed, RNAi-mediated depletion of Mbd3 led to an epithelial morphology of M3 clone cells with increased expression of E-cad and Cldn4, accompanied by reduced expression of Vim, Fn1, and transcription factors Zeb1, Snail, and Twist1 but not N-cad and Zeb2 (Fig. 4a–c, Supplementary Fig. S4a). Furthermore, the lack of Mbd3 expression in M3 clone cells provoked the conversion of mesenchymal stress fibers into epithelial cortical actin, a reduction in Vim expression and the localization of the epithelial markers E-cad and ZO-1 at cell–cell junctions (Fig. 4d). In contrast, stable depletion of Mbd3 in Py2T-LT cells did neither affect their mesenchymal cell morphology

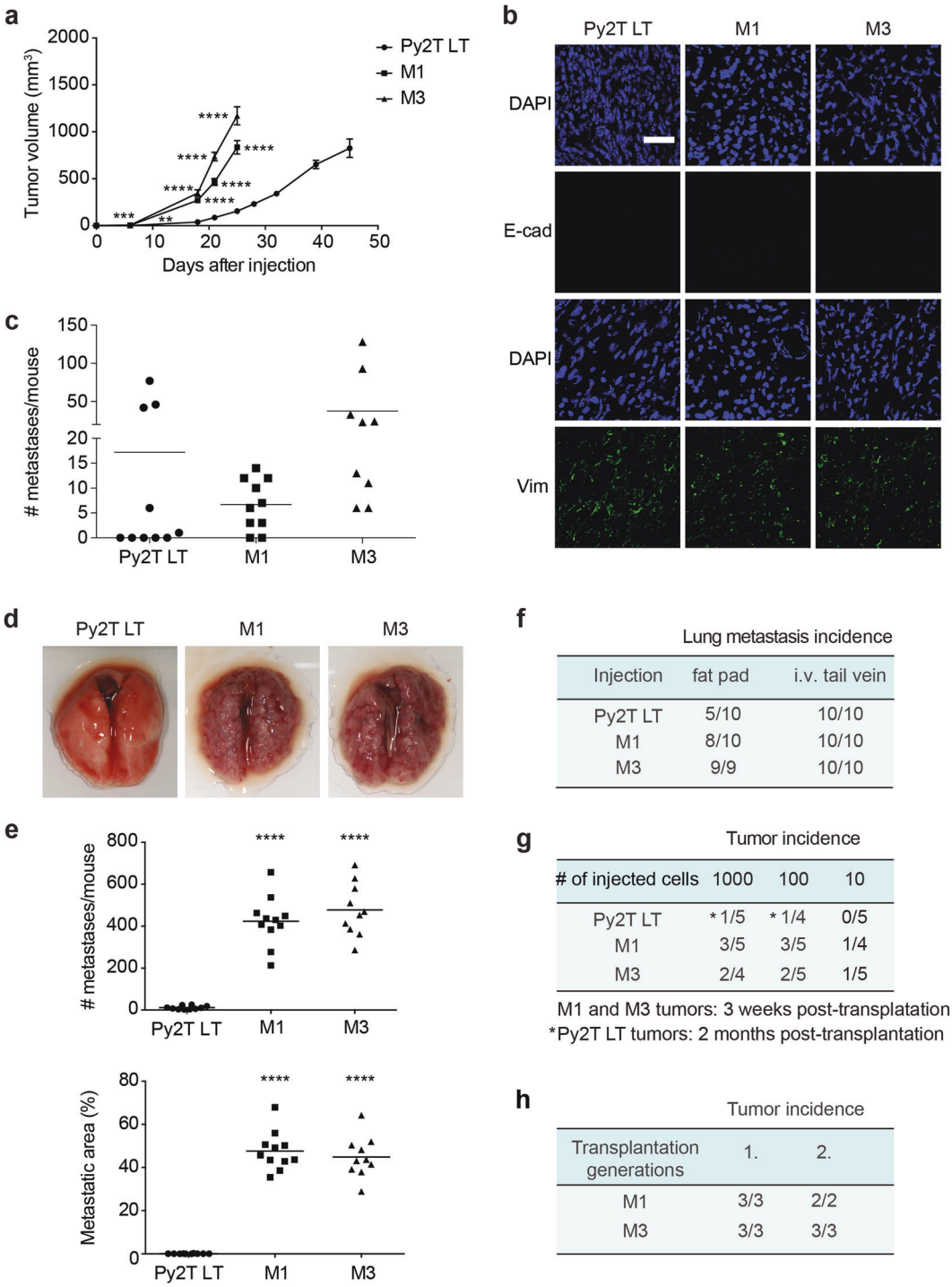

f

Lung metastasis incidence		
Injection	fat pad	i.v. tail vein
Py2T LT	5/10	10/10
M1	8/10	10/10
M3	9/9	10/10

g

Tumor incidence			
# of injected cells	1000	100	10
Py2T LT	*1/5	*1/4	0/5
M1	3/5	3/5	1/4
M3	2/4	2/5	1/5

M1 and M3 tumors: 3 weeks post-transplatation
*Py2T LT tumors: 2 months post-transplantation

h

Tumor incidence		
Transplantation generations	1.	2.
M1	3/3	2/2
M3	3/3	3/3

nor marker expression (Fig. 4a–d, Supplementary Fig. S4a). Transient depletion of Mbd3 by the transfection of siRNAs elicited similar changes in EMT marker expression and subcellular localization in M3 clone cells, yet at lower efficiency (Supplementary Fig. S4b–e). Moreover, depletion of MBD3 in mesenchymal, metastatic MDA-MB-231-LM2 human breast carcinoma cells led to a substantial increase in E-cad, yet with no detectable changes in Vim protein levels (Supplementary Fig. S4f). Taken together these results indicate that Mbd3 plays a critical role in sustaining the mesenchymal state not only in murine M clone cells but also in MDA-MB-231-LM2 human breast cancer cells.

Using RNA sequencing we compared the genes that are differentially expressed between shControl and shMbd3-expressing M3 clone cells (shMbd3 vs. shControl) to the

◀ **Fig. 2** Tumorigenicity of irreversible M clone cells. **a** Primary tumor growth in the mammary fat pad of female immunodeficient NOD/scid; common γ receptor$^{-/-}$ (NSG) mice transplanted with 10^5 cells of Py2T-LT cells and M1 and M3 clone cells. Data are displayed as mean tumor volumes ± SEM. **b** Immunofluorescence staining of tumors formed by Py2T-LT cells and M1 and M3 clone cells for E-cadherin (E-cad) and vimentin. DAPI staining was used to visualize nuclei. Scale bar, 50 µm. **c** Numbers of lung metastases per mouse transplanted orthotopically with Py2T-LT cells and M1 and M3 clone cells as described in **a**. **d** Representative macroscopic photographs of lungs taken 17 days post injection of 10^5 Py2T-LT cells or M1 and M3 clone cells into the tail vein of NSG mice. Means of the numbers of metastases and the percentages of the metastasis area per lung tissue area per mouse were quantified. **e** Quantification of the incidence and area of lung metastasis in the mice described in **d**. **f** Comparison of the incidence of lung metastasis of Py2T-LT cells and M1 and M3 clone cells injected into the mammary fat pad or intravenously into the tail vein. **g** Tumor incidence assessed by transplantation of Py2T-LT cells or M1 and M3 clone cells in limiting dilutions (1000, 100, 10 cells) into the mammary fat pads of female immunodeficient Rag$^{-/-}$; common γ receptor$^{-/-}$ (RG) mice. * represents the delayed tumor formation by Py2T-LT cells as compared with tumors initiated by M1 and M3 clone cells. The experiment was terminated 191 days post injection. **h** Tumor incidence of serial transplantation of fragments of tumors formed by M1 and M3 clone cells in the limiting dilution assay described in **f**. Statistical significance was calculated using a Mann–Whitney *U* test. $^{**}P < 0.01$; $^{***}P < 0.001$; $^{****}P < 0.0001$

genes that are differentially expressed between Py2T-LT and M3 clone cells (M3 vs. Py2T-LT) and identified 1351 genes to be specific for the Mbd3-dependent stable mesenchymal state (Supplementary Fig. S4g). Interestingly, the majority of these genes (940 out of 1351) were oppositely regulated by the depletion of Mbd3 (Supplementary Fig. S4h). These results indicate that Mbd3 affects a wide range of genes to maintain the irreversible mesenchymal state of M clone cells.

The transcription factors Snail1 and 2 [43, 44], Zeb1 [45–47], Zeb2 [47, 48], and Twist [49, 50] have been shown to regulate EMT by direct transcriptional repression of E-cad, in part by forming a complex with Mi2/NuRD [19–21]. Therefore, we analyzed the mRNA and protein expression levels of EMT markers and Mbd3 in Snail1, Zeb1, Zeb2, and Twist1-depleted Py2T-LT and M clone cells. The depletion of Zeb1, but not Snail1, Zeb2, and Twist1 led to an increase in mRNA and protein expression levels of E-cad in Py2T-LT and M clone cells, yet without reducing the expression of mesenchymal markers or of Mbd3 (Supplementary Fig. S5a–l, S6). These results indicate that Zeb1 represses E-cad in both reversible and irreversible EMT cells.

Tet2 is required for the maintenance of the mesenchymal cell state

Motivated by the report that 5hmC was critical for the recruitment of the Mbd3/NuRD complex to its target genes in embryonic stem cells [28], we assessed whether Tet family hydroxylases played a role in maintaining the mesenchymal phenotype of M clone cells. Consistent with the report that Mbd3 specifically enhanced the enzymatic activity of Tet2 but not Tet1 and Tet3 [51], stable shRNA or transient siRNA-mediated depletion of Tet2 in M3 clone cells provoked their conversion to an epithelial cell morphology with elevated expression of E-cad and Cldn4 and reduced expression of Vim, Fn1, N-cad, and Zeb1 (Fig. 5a–c; Supplementary Fig. S7a,b). Moreover, the localization of E-cad and ZO-1 at cell–cell junctions, accompanied by cortical actin formation and reduced Vim expression was apparent in shTet2-expressing or siRNA-transfected M3 clone cells (Fig. 5d; Supplementary Fig. S7c). In contrast, knockdown of Tet2 in Py2T-LT cells did neither affect cell morphology nor EMT marker expression (Fig. 5a–d; Supplementary Fig. S7a–c). Depletion of Snail1, Zeb1, Zeb2, and Twist1 in Py2T-LT and M clone cells revealed that only Snail1 affected the expression of Tet2 in M clone cells (Supplementary Fig. S5a–l). Together, the results indicate that Tet2 is a critical player in the maintenance of a mesenchymal state in irreversible EMT cells.

Comparative gene expression analysis by RNA sequencing revealed that 1116 genes were directly affected by Tet2 when comparing genes changing in their expression upon depletion of Tet2 in M3 clone cells (shTet2 vs shControl) and genes differentially expressed between M3 clone cells and Py2T-LT cells (M3 vs Py2T-LT) (Supplementary Fig. S7d). Similar to the depletion of Mbd3, the majority of these genes (760 out of 1116) were oppositely regulated by the loss of Tet2 expression (Supplementary Fig. S7e), indicating a profound function of Tet2 and Mbd3 in maintaining a mesenchymal cell state.

Combinatorial targeting of HDACs and Mbd3 or Tet2

We next tested whether a combination of pharmacological HDAC inhibition and the ablation of Mbd3 or Tet2 expression provided an additive effect in the reversion of M clone cells to an epithelial state. The combination of the shRNA-mediated ablation of Tet2 or Mbd3 with the treatment with CI994 in M3 clone cells showed an increased E-cad expression accompanied by the loss of Vim and Fn1 expression, as compared with the individual treatments alone (Fig. 6a). Interestingly, the ablation of either Tet2 or Mbd3 caused an upregulation of H3 acetylation levels even in the absence of CI994, indicating the depletion of Tet2 and Mbd3 reduced HDAC activity (Fig. 6a), likely by disrupting Mbd3/NuRD complexes. M3 clone cells depleted of Tet2 or Mbd3 expression already showed an epithelial cell morphology and change in EMT marker expression which only moderately increased upon combination treatment with CI994 (Fig. 6a, b; Supplementary Fig. S8a). Yet, the combination treatment induced a more efficient localization of E-

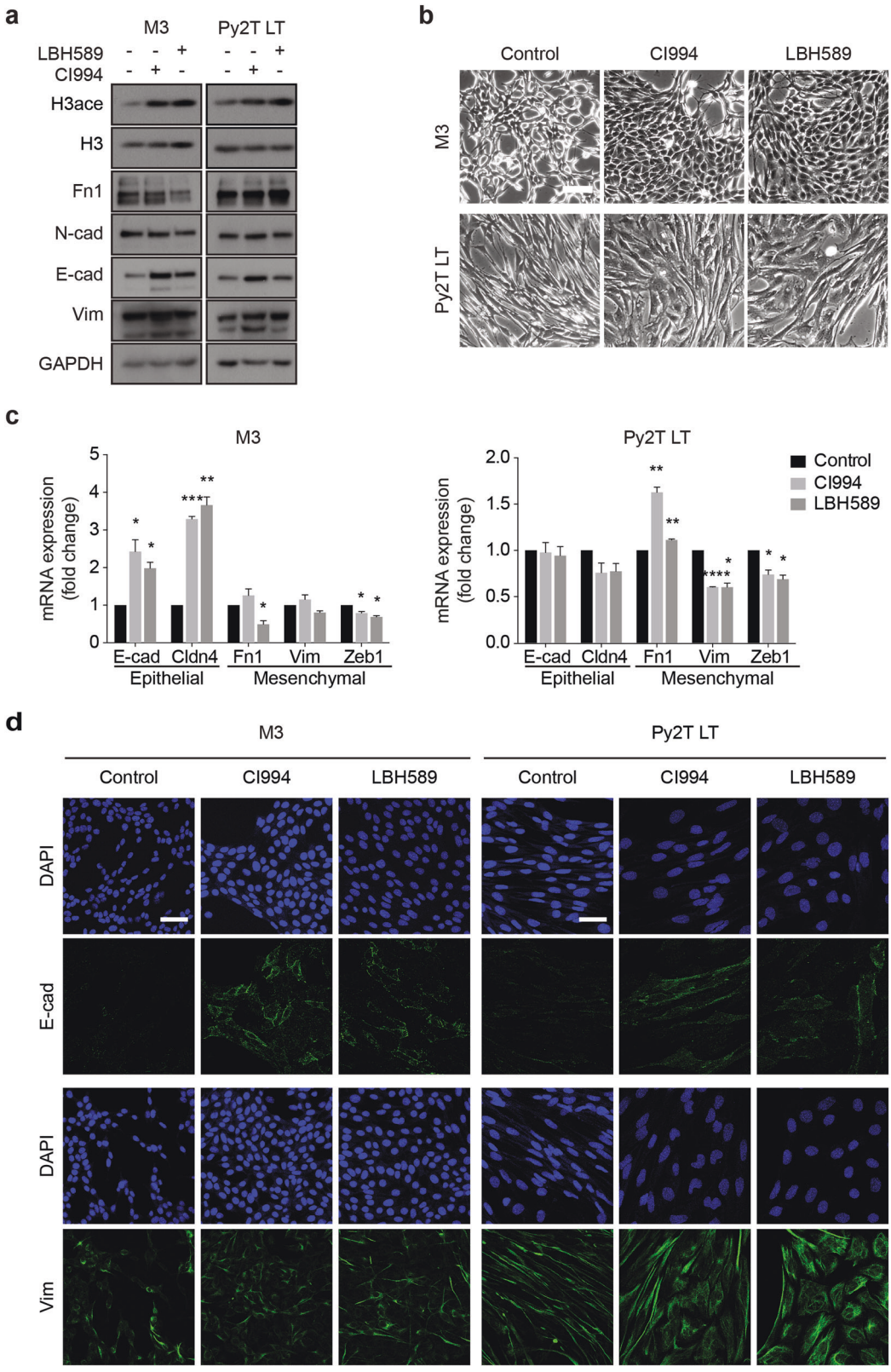

cad and ZO-1 at cell–cell junctions and the formation of cortical actin while enhancing a reduction in Vim expression, as compared with the treatments alone (Fig. 6c, Supplementary Fig. S8b). In contrast, while the combinatorial treatment of Py2T-LT cells induced a slight increase in E-cad expression and reduction in Fn1 and N-cad expression

◀ **Fig. 3** HDAC inhibition induces a partial MET in M clone cells. **a** The protein levels of acetylated H3 (H3ace), fibronectin (Fn1), N-cadherin (N-cad), E-cadherin (E-cad), and vimentin (Vim) in M3 clones and Py2T-LT cells exposed or not to HDAC inhibitors (2 μM Tacedinaline/CI994 or 10 nM Panobinostat/LBH589) for 72 h were determined by immunoblotting. Immunoblotting for total H3 and GAPDH was used as a loading control. **b** Morphology of M3 clone cells and Py2T-LT cells treated with 2 μM CI994 and 10 nM LBH589 for 72 h as evaluated by phase contrast microscopy. Scale bar, 100 μm. **c** Quantitative RT-PCR analysis of the mRNA levels of E-cadherin (E-cad), Claudin4 (Cldn4), fibronectin (Fn1), vimentin (Vim), and Zeb1 in M3 clone cells and Py2T-LT cells treated with CI994 (2 μM) and LBH589 (10 nM) for 72 h. Fold changes are related to mRNA levels in cells treated with DMSO diluent. Data are displayed as mean ± SEM. Statistical values were calculated using a paired, two-tailed *t*-test. $*P < 0.05$; $**P < 0.01$, $***P < 0.001$; $****P < 0.0001$. **d** Confocal immunofluorescence microscopy analysis of the expression of the epithelial marker E-cadherin (E-cad) and the mesenchymal marker vimentin (Vim) in M3 clone cells and Py2T-LT cells in the absence and presence of HDAC inhibitors CI994 (2 μM) and LBH589 (10 nM) for 72 h. Scale bars, 50 μm

(Fig. 6a), it did neither provoke the localization of E-cad and ZO-1 at cell–cell junctions nor reduce mesenchymal Vim expression and actin stress fiber formation (Fig. 6c, Supplementary Fig. S8b). Overall, the results suggest that a functional Mbd3/NuRD complex together with HDAC and Tet2 hydroxylase activities are required for the maintenance of a stable mesenchymal cell state.

RNA sequencing identified 367 genes that were differentially expressed upon treatment of M3 clone cells with the HDAC inhibitor CI994 or by the depletion of Mbd3 or Tet2 alone (Supplementary Fig. S9a). Further, 784 genes were differentially regulated between Mbd3 or Tet2 depletion alone and Mbd3 or Tet2 depletion in combination with CI994 treatment (Supplementary Fig. S9a). Finally, comparison of the 367 genes shared between CI994, shMbd3, and shTet2 treatments and the 784 genes that were assigned to the additive effect of HDAC inhibition in combination with Mbd3 and Tet2 depletion identified 92 genes which changed in their expression by all the treatments leading to an epithelial reversion of M clone cells. We hypothesize that the 92 genes could be responsible for the additive effect of HDAC inhibition and Mbd3 or Tet2 depletion during MET of M clone cells and we refer to this list of genes as "induced MET (iMET)" gene signature (Supplementary Fig. S9a).

We next assessed whether the iMET genes were also differentially regulated during MET of a reversible EMT system. RNA-sequencing was performed at early, middle, and late time points of MET of Py2T-LT cells upon TGFβ withdrawal (Py2T MET; Supplementary Table S1). Differentially expressed genes during the time course of Py2T MET cells were then compared with the 92 gene iMET signature (Supplementary Fig. S9b; Supplementary Table S1). This analysis revealed not only common but also distinct gene expression patterns between the iMET gene signature and the genes changing during the reversible MET time course suggesting that an irreversible and a reversible EMT are distinct processes.

Tet2 and Mbd3 are required for primary tumor growth and metastasis

The combinatorial role of Tet2, Mbd3, and HDACs in maintaining the mesenchymal phenotype of M clone cells in vitro motivated us to test whether these epigenetic modifiers also play a role during primary tumor growth and metastasis formation in vivo. M3 clone cells stably expressing shRNAs against Tet2 (shTet2), Mbd3 (shMbd3), and a non-targeting control-shRNA (shControl) were orthotopically implanted into the mammary fat pads of immunodeficient NSG mice. When tumors were first palpable, daily treatment with CI994 was initiated (35 mg/kg; i.p.). The efficient ablation of Tet2 and Mbd3 led to a significant decrease in primary tumor growth and tumor weights. The combination with CI994 treatment, which enhanced H3 acetylation levels, caused a further significant reduction in tumor growth and tumor weights as compared with the vehicle-treated cohorts (Fig. 7a, b, Supplementary Fig. S10a). In addition, the combinatorial treatment with CI994 enhanced the upregulation of epithelial markers and the downregulation of mesenchymal markers in Tet2 and Mbd3-depleted primary tumors (Supplementary Fig. S10b).

The ablation of Tet2 and Mbd3 also significantly reduced the number and the area of metastasis in the lungs of the tumor bearing mice, even when the number of metastases was normalized to the decreased primary tumor weights observed with the depletion of Tet2 or Mbd3 (metastatic index; Fig. 7c). Remarkably, no metastatic lesions could be detected in mice implanted with Mbd3 knockdown M3 clone cells with or without CI994 treatment. In contrast, the pharmacological inhibition of HDACs by itself did not cause a significant reduction in the number and area of lung metastasis nor in the metastatic index.

To assess the generality of our findings for human breast cancer, we investigated the functional contribution of HDAC inhibition and Mbd3 to primary tumor growth and metastasis formation using MDA-MB-231-LM2 (LM2) human breast cancer cells, a gold standard xenograft transplantation model of efficient lung metastasis [52]. Control (shControl) and MBD3-depleted (shMBD3-2 and shMBD3-5) LM2 cells (Supplementary Fig. S3d) were orthotopically implanted into the mammary fat pads of NSG mice. When the tumors were palpable, daily treatment with CI994 was initiated (35 mg/kg; i.p.). The ablation of MBD3 in MBD3-5 cells led to a significant decrease in the primary tumor growth, which was less profound, yet still significant with MBD3-2 cells. The combination with CI994 treatment caused an increase in tumor growth and tumor weights as compared with the vehicle-treated cohorts (Fig. 7d).

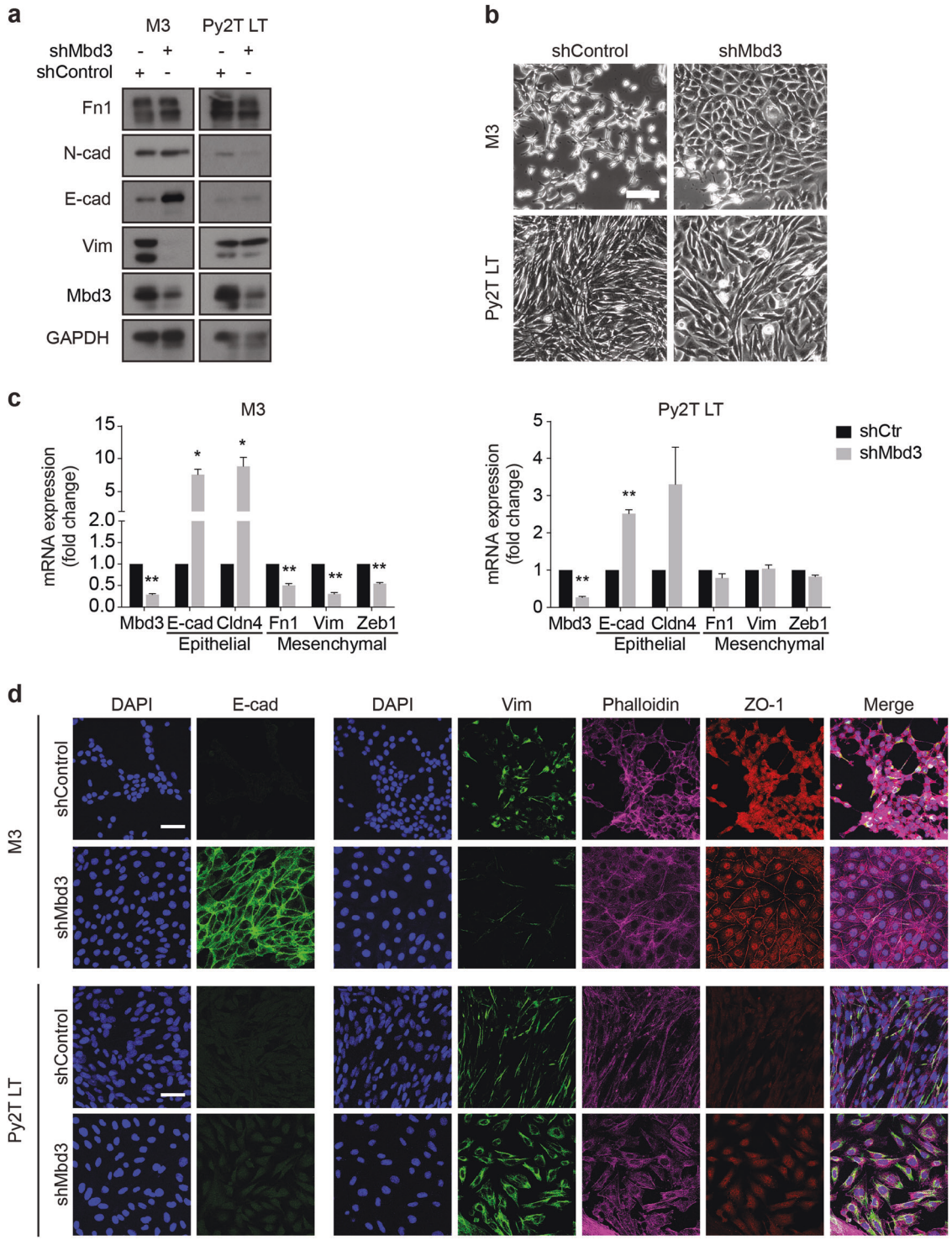

Fig. 4 The Mbd3/NuRD complex is required for the maintenance of a mesenchymal cell state. **a** The protein levels of fibronectin (Fn1), N-cadherin (N-cad), E-cadherin (E-cad), vimentin (Vim), and Mbd3 were evaluated by immunoblotting in M3 clone cells and in Py2T-LT cells expressing either shControl or shMbd3. Immunoblotting for GAPDH was used as a loading control. **b** Phase-contrast microscopy of M3 clone cells and Py2T-LT cells stably expressing shControl or shMbd3. Scale bar, 100 µm. **c** Quantitative RT-PCR analysis of the mRNA levels of Mbd3, E-cadherin (E-cad), Claudin4 (Cldn4), fibronectin (Fn1), vimentin (Vim), and Zeb1 in M3 clone cells and Py2T-LT cells expressing shMbd3. Fold changes are related to M3 clone cells and Py2T-LT cells expressing shControl. Data are displayed as mean ± SEM. Statistical values were calculated using a paired, two-tailed *t*-test. $*P < 0.05$; $**P < 0.01$. **d** Confocal immunofluorescence microscopy analysis of the expression and localization of the epithelial markers E-cadherin (E-cad) and ZO-1 and the mesenchymal marker vimentin (Vim) in M3 clone cells and Py2T-LT cells expressing either shControl or shMbd3. Phalloidin and DAPI staining visualize the actin cytoskeleton and nuclei, respectively. Scale bars, 50 µm

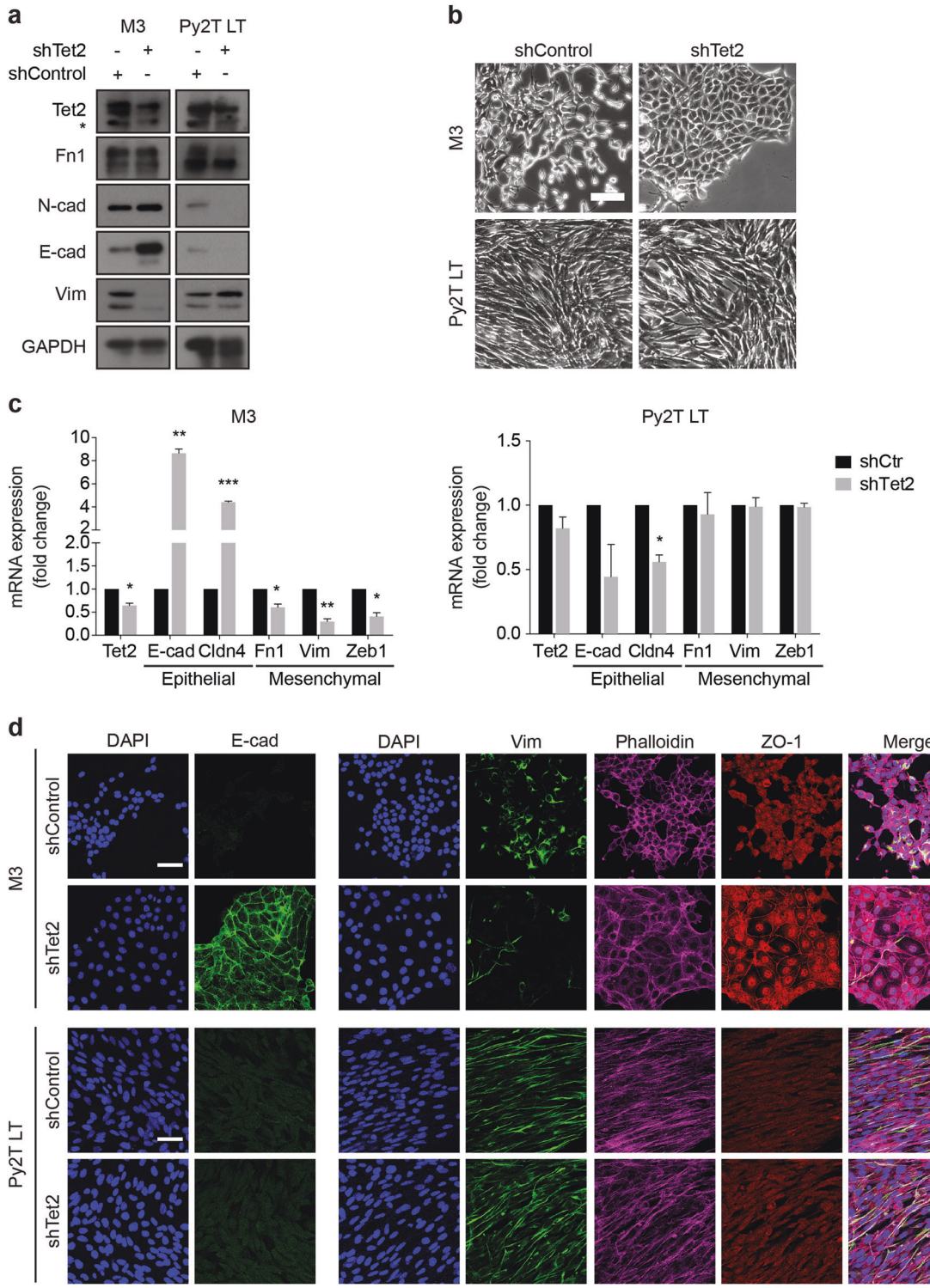

Notably, the number and the area of metastasis in the lungs of shMBD3-2 and shMBD3-5 tumor-bearing mice were significantly reduced (Fig. 7e). The inhibition of HDACs by itself did not cause a significant reduction in the number and surface area of lung metastasis nor in the metastatic index.

Altogether, these findings indicate that Tet2 and the Mbd3/NuRD complex play a pivotal role during primary tumor growth and metastasis formation of highly metastatic human and murine breast cancer cells exhibiting an irreversible EMT.

◀ **Fig. 5** Tet2 is required for the maintenance of a mesenchymal cell state. **a** Protein levels of Tet2, fibronectin (Fn1), N-cadherin (N-cad), E-cadherin (E-cad), and vimentin (Vim) were determined by immunoblotting in M3 clone cells and Py2T-LT cells expressing either shControl or shTet2. Immunoblotting for GAPDH was used as a loading control. *indicates a non-specific protein band stained by anti-Tet2 antibodies. **b** Phase-contrast microscopy of M3 clone cells and Py2T-LT cells expressing shControl or shTet2. Scale bar, 100 µm. **c** Quantitative RT-PCR analysis of the mRNA levels of Tet2, E-cadherin (E-cad), Claudin4 (Cldn4), fibronectin (Fn1), vimentin (Vim), and Zeb1 mRNA levels in M3 clone cells and Py2T-LT cells expressing shTet2. Fold changes are related to cells expressing shControl. Data are displayed as mean ± SEM. Statistical values were calculated using a paired, two-tailed *t*-test. $*P < 0.05$; $**P < 0.01$; $***P < 0.001$. **d** Confocal immunofluorescence microscopy analysis of the expression and localization of E-cadherin (E-cad) and ZO-1 and vimentin (Vim) in M3 clone cells and Py2T-LT cells expressing either shControl or shTet2. Phalloidin and DAPI staining visualize the actin cytoskeleton and nuclei, respectively. Scale bars, 50 µm

Discussion

We have set out to identify molecular mechanisms underlying the reversibility and irreversibility of EMT in murine breast cancer cells. We have used Py2T murine breast cancer cells that undergo reversible EMT upon stimulation with TGFβ to generate derivatives that maintain a stable mesenchymal phenotype upon normal culture conditions (M clones). The generation of the mesenchymal Py2T-LT cells is induced by exogenous TGFβ in the culture medium, and the cells are clearly dependent on the TGFβ inducive activity to maintain their mesenchymal cellular state. In contrast, M clone cells have been established in the complete absence of any exogenous TGFβ and remain in their mesenchymal state without any addition of TGFβ.

We find that M clone cells, but not Py2T-LT cells, can be forced to undergo MET when treated with HDAC inhibitors or when depleted of Mbd3 or Tet2 expression. Notably, while the combination of pharmacological HDAC inhibition and the genetic depletion of Mbd3 or Tet2 shows an additive effect in the repression of primary tumor growth, this additive effect is not apparent in the inhibition of lung metastasis. The results indicate that the Mbd3/NuRD complex containing HDACs and Tet2 may play a critical role in defining epithelial–mesenchymal plasticity during EMT and MET and during the metastatic process. Combinatorial targeting of its components may thus offer an efficient approach to interfere with malignant disease.

While previous studies have mainly focused on HDACs' functional contributions to cancer cell apoptosis, proliferation and angiogenesis, results on the role of HDACs in epithelial-mesenchymal plasticity have been conflicting. Some reports show that HDAC inhibition induces an EMT in cancer cells [53, 54], while in other cancer cell types it promotes a partial MET state [10, 12]. Furthermore, HDAC inhibition represses drug resistance of cancer cells forced to undergo an EMT by the expression of the transcription factor Zeb1 [40]. Consistent with the latter reports, we find that HDAC inhibition causes a partial MET phenotype in irreversible EMT cells, whereas no marked effects are observed in reversible EMT cells. Notably, while HDAC inhibition represses primary tumor growth with a significant upregulation of epithelial marker expression, it has no discernable effect on metastasis formation.

Irreversible EMT M clone cells exhibit a higher capacity in tumor initiation, tumor growth, and colonization in the lung as compared with Py2T LT cells. EMT score analysis [55] shows that M3 clone cells were confined in the partial (hybrid) EMT state, whereas Py2T LT cells exhibited a full EMT phenotype (Supplementary Fig. S11). In fact, 6624 genes are found differentially expressed between Py2T-LT cells and M clone cells, suggesting that the irreversible M clone cells significantly differ from reversible Py2T-LT cells, although they both originated from Py2T cells. Our data is consistent with the recent findings implicating an important role of partial (hybrid) EMT in tumor aggressiveness, metastasis, cancer stemness, and drug resistance compared with the full EMT state [56–59] and indicating that a partial EMT could be a stable state rather than a metastable state [60]. EMT score analysis also showed that treatment with HDAC inhibitors did not affect the E/M state of M3 clone cells, whereas the depletion of Tet2 or Mbd3 with or without HDAC inhibitor treatment induced a more epithelial phenotype of mesenchymal M clone cells (Supplementary Fig. S11). This analysis may explain why HDAC inhibition by itself was not effective to prevent metastasis, whereas Tet2 and Mbd3 dramatically reduced metastasis formation, not only in the M clone murine mesenchymal breast cancer cells but also in highly metastatic MDA-MB-231-LM2 human breast cancer cells. Hence, we conclude that Tet2 and Mbd3 drive changes in cancer cell state from a highly aggressive partial EMT state to a less aggressive epithelial state.

Here, we demonstrate an important regulatory role of the epigenetic modifiers Mbd3/NuRD and Tet2 in the regulation of cell state transitions and of primary tumor growth and metastasis by their ability to affect the expression of a wide range of genes. Notably, we have identified a 92 gene iMET signature representing genes that are differentially regulated during MET of irreversible EMT cells induced by a combination of HDAC inhibition and depletion of Mbd3 and/or Tet2. While potent pharmacological inhibitors against HDACs have been developed and are in clinical trials, their clinical efficacy appears disappointing. Our work suggests that HDAC inhibition should be combined with the inhibition of Mbd3/NuRD and Tet hydroxylases. Unfortunately, efficient inhibitors of Tet hydroxylases and of the Mbd3/NuRD complex are only in development or are lacking [61]. Due to their pleiotropic mode of action and their reversible

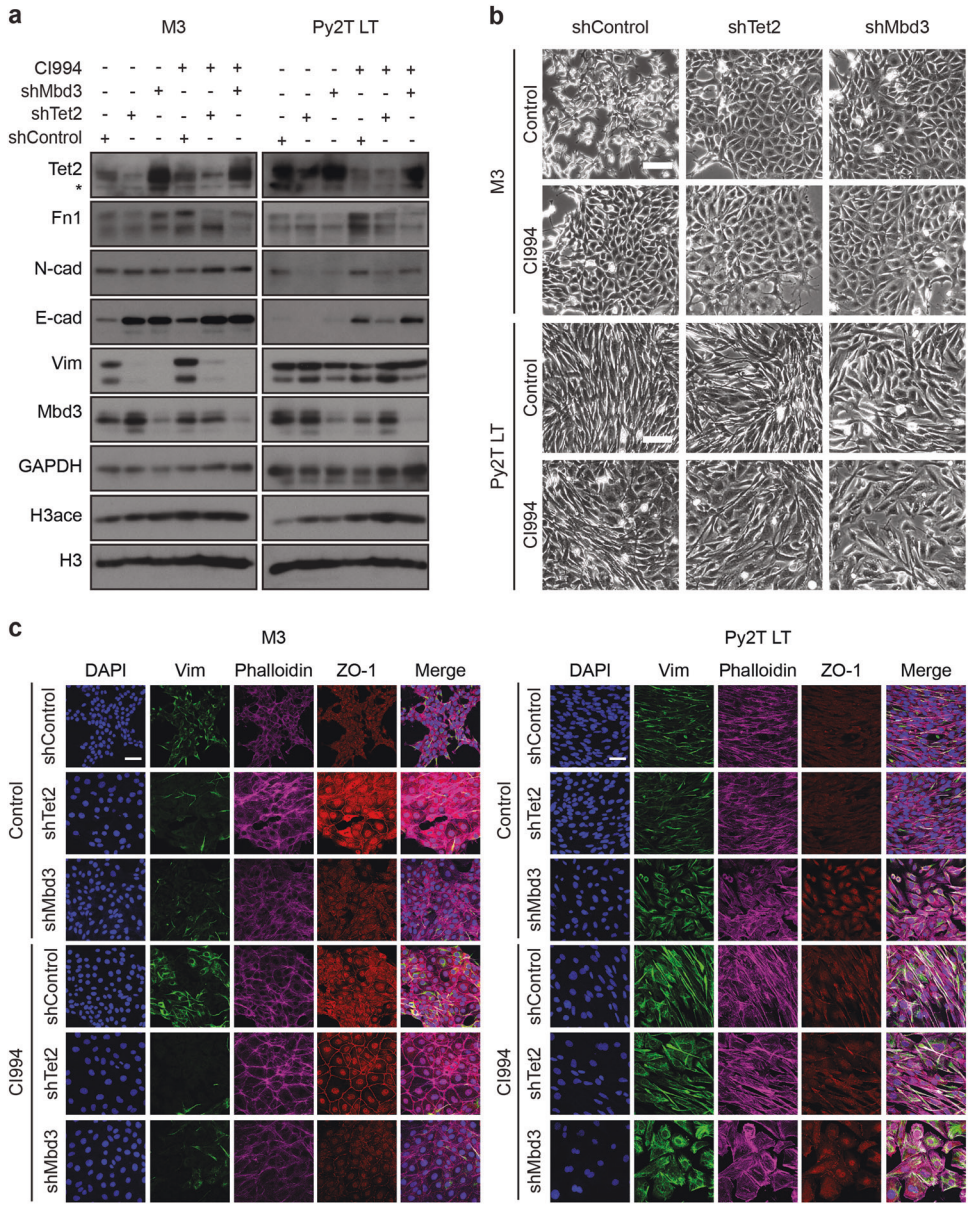

Fig. 6 Combination of the depletion of Mbd3 or Tet2 expression with HDAC inhibition potentiates an MET of stable mesenchymal cells. **a** Protein levels of Tet2, fibronectin (Fn1), N-cadherin (N-cad), E-cadherin (E-cad), vimentin (Vim), and Mbd3, as determined by immunoblotting of M3 clone cells and Py2T-LT cells stably expressing shControl, shTet2, or shMbd3 and cultured in the absence or presence of 2 µM CI994 for 72 h. Immunoblotting for GAPDH was used as a loading control. *indicates a non-specific protein band bound by anti-Tet2 antibodies. **b** Phase-contrast microscopy of M3 clone cells and Py2T-LT cells expressing shControl, shTet2, or shMbd3 and cultured in the absence or presence of 2 µM CI994. Scale bars, 100 µm. **c** Confocal immunofluorescence microscopy analysis of the localization and expression of ZO-1 and vimentin (Vim) in M3 clone cells and Py2T-LT cells expressing shControl, shTet2, or shMbd3 and cultured in the absence or presence of 2 µM CI994 for 72 h. Phalloidin and DAPI staining visualize the actin cytoskeleton and nuclei, respectively. Scale bars, 50 µm

nature, these epigenetic modifiers are attractive targets for the development of novel cancer therapies.

Material and methods

For further details see Supplementary Information.

Cell lines

Py2T cells [33] and M clone cells were cultured in Dulbecco's modified Eagle's medium (DMEM) and MDA-MB-231-LM2 cells [52] were cultured in DMEM/ Nutrient mixture F-12 Ham (DMEM/F12) supplemented with glutamine, penicillin, streptomycin, and 10% FBS (Sigma-Aldrich). Py2T cells were treated with 2 ng/ml TGFβ1 and the medium was replenished every 3 days. All cells were cultured at 37 °C with 5% CO_2 in a humid incubator.

In vitro irreversible EMT clones: M clones were generated by culturing in MEGM (mammary epithelial cell growth medium) supplemented with SupplementMix (PromoCell) and glutamine, penicillin, streptomycin, and 7% FBS (Sigma-Aldrich) for 3 months, when subpopulations of mesenchymal cells became apparent. Then, cells were transferred into DMEM supplemented with glutamine, penicillin, streptomycin, and 10% FBS (Sigma-Aldrich) and cultured for 2 months to select for stable mesenchymal subpopulations, which were subsequently isolated as single cells and expanded as cell clones.

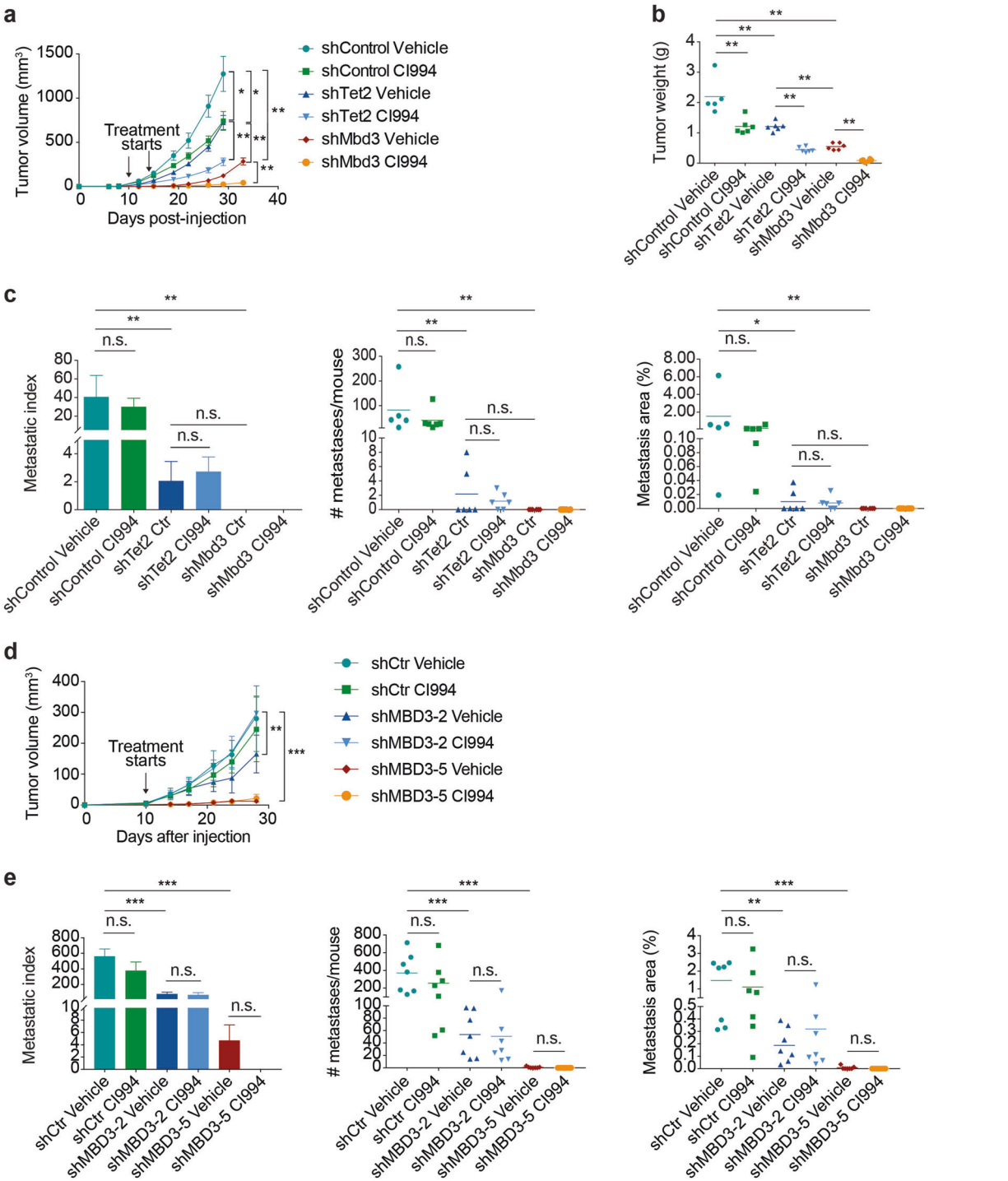

Inhibitor treatments: Py2T-LT cells and M clone cells were treated with 2 µM CI994 or 10 nM LBH589 for 3 days. M2 and M3 clones were treated with 5 µM DZNep, 2 µM Decitabine, or 100 nM TSA for 3 days. Py2T-LT cells and M3 clones were treated with 5 µM CI994 or 5 µM EPZ005687 for 6 days.

Primers used for quantitative RT-PCR are listed in Supplementary Table S2.

Pyro-sequencing primers are given in Supplementary Table S3.

Data availability

Further information and requests for resources and reagents should be directed to and will be fulfilled by the Lead Contact, Gerhard Christofori (gerhard.christofori@unibas.ch). The

◀ **Fig. 7** Depletion of Mbd3 or Tet2 expression in combination with HDAC inhibition efficiently represses primary tumor growth and lung metastasis. **a** 10^5 shControl, shTet2, and shMbd3-expressing M3 clone cells were transplanted into the mammary fat pads of immunodeficient female RG mice. When the tumors were palpable, mice were treated with HDAC inhibitor CI994 (35 mg/kg, i.p.), and tumor growth was measured over time. At least five mice were used for experimental cohort. Data are displayed as mean tumor volumes ± SEM. **b** The mice described in **a** were sacrificed after 29 days of treatment and tumor weights were assessed. **c** Metastatic spread of shControl, shTet2, and shMbd3-expressing M3 clone tumors treated with vehicle or HDAC inhibitor CI994 was determined by serial sectioning of the lungs of mice described in **a** and **b**. The metastatic index was calculated by the number of metastases divided by the primary tumor weights within the same mice (left panel). Mean of the number of metastases (middle panel) and metastatic area percentages per mouse were also quantified (right panel). **d** 10^6 MDA-MB-231-LM2 cells stably expressing shControl, shMBD3-2, and shMBD3-5 were transplanted into the mammary fat pads of immunodeficient female NSG mice. When the tumors were palpable, mice were treated with HDAC inhibitor CI994 (35 mg/kg, i.p.), and tumor growth was measured over time. At least seven mice were used for experimental cohort. Data are displayed as mean tumor volumes ± SEM. **e** Metastatic spread of MDA-MB-231-LM2 stably expressing shControl, shMBD3-2, and shMBD3-5 tumors treated with vehicle or HDAC inhibitor CI994 was determined by serial sectioning of the lungs of mice described in **d**. The metastatic index was calculated by the number of metastases divided by the primary tumor weights within the same mice (left panel). Mean of the number of metastases (middle panel) and metastatic area percentages per mouse were also quantified (right panel). Statistical significance was calculated using a Mann–Whitney *U* test. N.s., non-significant; $*P < 0.05$; $**P < 0.01$; $***P < 0.001$

RNA sequencing data are deposited at Gene Expression Omnibus (GEO accession number: GSE100553).

Acknowledgements We thank P. Schär and S. Weis (DBM Basel) for reagents and protocols, F. Noreen (DBM Basel) for pyrosequencing, C. Beisel (D-BSSE, ETH Zürich) for next generation RNA sequencing, P. Lorentz (DBM Basel) for excellent microscopy support, and Isabel Galm for technical support.

Funding This work was supported by the SystemsX.ch RTD project Cellplasticity, the SystemsX.ch MTD project MetastasiX, the Swiss National Science Foundation, and the Swiss Cancer League. MKJ was also supported by a training fellowship from the Gulf Coast Consortia on the Computational Cancer Biology Training Program (CPRIT Grant No. RP170593).

Author contributions ANK designed and performed the experiments, analyzed the data and wrote the paper; NS performed experiments for revision, RKRK performed bioinformatics analysis; HA performed animal experiments; HB analyzed animal experiments, DI-R performed Py2T MET Time-course, JTG, HL and MKJ performed EMT score analysis; and GC oversaw the project, designed experiments, analyzed the data and wrote the paper.

Compliance with ethical standards

Conflict of interest The authors declare that they have no conflict of interest.

Publisher's note Springer Nature remains neutral with regard to jurisdictional claims in published maps and institutional affiliations.

References

1. Hanahan D, Weinberg RA. Hallmarks of cancer: the next generation. Cell. 2011;144:646–74.
2. Thiery JP. Epithelial-mesenchymal transitions in tumour progression. Nat Rev Cancer. 2002;2:442–54.
3. Yang J, Weinberg RA. Epithelial-mesenchymal transition: at the crossroads of development and tumor metastasis. Dev Cell 2008;14:818–29.
4. Nieto MA. The ins and outs of the epithelial to mesenchymal transition in health and disease. Annu Rev Cell Dev Biol. 2011;27:347–76.
5. Diepenbruck M, Christofori G. Epithelial-mesenchymal transition (EMT) and metastasis: yes, no, maybe? Curr Opin Cell Biol. 2016;43:7–13.
6. Fantozzi A, Gruber DC, Pisarsky L, Heck C, Kunita A, Yilmaz M, et al. VEGF-mediated angiogenesis links EMT-induced cancer stemness to tumor initiation. Cancer Res. 2014;74:1566–75.
7. McDonald OG, Wu H, Timp W, Doi A, Feinberg AP. Genome-scale epigenetic reprogramming during epithelial-to-mesenchymal transition. Nat Struct Mol Biol. 2011;18:867–74.
8. Tam WL, Weinberg RA. The epigenetics of epithelial-mesenchymal plasticity in cancer. Nat Med. 2013;19:1438–49.
9. Glozak MA, Seto E. Histone deacetylases and cancer. Oncogene. 2007;26:5420–32.
10. Tate CR, Rhodes LV, Segar HC, Driver JL, Pounder FN, Burow ME, et al. Targeting triple-negative breast cancer cells with the histone deacetylase inhibitor panobinostat. Breast Cancer Res. 2012;14:R79.
11. Srivastava RK, Kurzrock R, Shankar S. MS-275 sensitizes TRAIL-resistant breast cancer cells, inhibits angiogenesis and metastasis, and reverses epithelial-mesenchymal transition in vivo. Mol Cancer Ther. 2010;9:3254–66.
12. Tang HM, Kuay KT, Koh PF, Asad M, Tan TZ, Chung VY, et al. An epithelial marker promoter induction screen identifies histone deacetylase inhibitors to restore epithelial differentiation and abolishes anchorage independence growth in cancers. Cell Death Discov. 2016;2:16041.
13. Grozinger CM, Schreiber SL. Deacetylase enzymes: biological functions and the use of small-molecule inhibitors. Chem Biol. 2002;9:3–16.
14. Denslow SA, Wade PA. The human Mi-2/NuRD complex and gene regulation. Oncogene. 2007;26:5433–8.
15. Hayakawa T, Nakayama J. Physiological roles of class I HDAC complex and histone demethylase. J Biomed Biotechnol. 2011;2011:129383.
16. Yang Y, Huang W, Qiu R, Liu R, Zeng Y, Gao J, et al. LSD1 coordinates with the SIN3A/HDAC complex and maintains sensitivity to chemotherapy in breast cancer. J Mol Cell Biol. 2018;10:285–301.
17. Wang Y, Zhang H, Chen Y, Sun Y, Yang F, Yu W, et al. LSD1 is a subunit of the NuRD complex and targets the metastasis programs in breast. Cancer Cell. 2009;138:660–72.
18. Peinado H, Ballestar E, Esteller M, Cano A. Snail mediates E-cadherin repression by the recruitment of the Sin3A/Histone deacetylase 1 (HDAC1)/HDAC2 complex. Mol Cell Biol. 2004;24:306.
19. Fujita N, Jaye DL, Kajita M, Geigerman C, Moreno CS, Wade PA. MTA3, a Mi-2/NuRD complex subunit, regulates an invasive growth pathway in breast. Cancer Cell. 2003;113:207–19.
20. Fu J, Qin L, He T, Qin J, Hong J, Wong J, et al. The TWIST/Mi2/NuRD protein complex and its essential role in cancer metastasis. Cell Res. 2011;21:275–89.
21. Verstappen G, van Grunsven LA, Michiels C, Van de Putte T, Souopgui J, Van Damme J, et al. A typical Mowat–Wilson patient

confirms the importance of the novel association between ZFHX1B/SIP1 and NuRD corepressor complex. Hum Mol Genet. 2008;17:1175–83.
22. Lai AY, Wade PA. Cancer biology and NuRD: a multifaceted chromatin remodelling complex. Nat Rev Cancer. 2011; 11:588–96.
23. Kaji K, Caballero IM, MacLeod R, Nichols J, Wilson VA, Hendrich B. The NuRD component Mbd3 is required for pluripotency of embryonic stem cells. Nat Cell Biol. 2006;8:285–92.
24. Kaji K, Nichols J, Hendrich B. Mbd3, a component of the NuRD co-repressor complex, is required for development of pluripotent cells. Development. 2007;134:1123–32.
25. Rais Y, Zviran A, Geula S, Gafni O, Chomsky E, Viukov S, et al. Deterministic direct reprogramming of somatic cells to pluripotency. Nature. 2013;502:65–70.
26. Saito M, Ishikawa F. The mCpG-binding domain of human MBD3 does not bind to mCpG but interacts with NuRD/Mi2 components HDAC1 and MTA2. J Biol Chem. 2002; 277:35434–9.
27. Fraga MF, Ballestar E, Montoya G, Taysavang P, Wade PA, Esteller M. The affinity of different MBD proteins for a specific methylated locus depends on their intrinsic binding properties. Nucleic Acids Res. 2003;31:1765–74.
28. Yildirim O, Li R, Hung J-H, Chen Poshen B, Dong X, Ee L-S, et al. Mbd3/NURD complex regulates expression of 5-hydroxymethylcytosine marked genes in embryonic stem cells. Cell. 2011;147:1498–510.
29. Tahiliani M, Koh KP, Shen Y, Pastor WA, Bandukwala H, Brudno Y, et al. Conversion of 5-methylcytosine to 5-hydroxymethylcytosine in mammalian DNA by MLL partner TET1. Science. 2009;324:930–5.
30. Cimmino L, Abdel-Wahab O, Levine Ross L, Aifantis I. TET family proteins and their role in stem cell differentiation and transformation. Cell Stem Cell. 2011;9:193–204.
31. Baubec T, Ivánek R, Lienert F, Schübeler D. Methylation-dependent and -independent genomic targeting principles of the MBD protein family. Cell. 2013;153:480–92.
32. Hu X, Zhang L, Mao S-Q, Li Z, Chen J, Zhang R-R, et al. Tet and TDG mediate DNA demethylation essential for mesenchymal-to-epithelial transition in somatic cell reprogramming. Cell Stem Cell. 2014;14:512–22.
33. Waldmeier L, Meyer-Schaller N, Diepenbruck M, Christofori G. Py2T murine breast cancer cells, a versatile model of TGFβ-induced EMT in vitro and in vivo. PLoS ONE. 2012;7: e48651.
34. Dumont N, Wilson MB, Crawford YG, Reynolds PA, Sigaroudinia M, Tlsty TD. Sustained induction of epithelial to mesenchymal transition activates DNA methylation of genes silenced in basal-like breast cancers. Proc Natl Acad Sci. 2008;105:14867–72.
35. Crea F, Paolicchi E, Marquez VE, Danesi R. Polycomb genes and cancer: time for clinical application? Crit Rev Oncol/Hematol. 2012;83:184–93.
36. Tiwari N, Tiwari Vijay K, Waldmeier L, Balwierz Piotr J, Arnold P, Pachkov M, et al. Sox4 is a master regulator of epithelial-mesenchymal transition by controlling Ezh2 expression and epigenetic reprogramming. Cancer Cell. 2013;23:768–83.
37. Zhang N, Liu Y, Wang Y, Zhao M, Tu L, Luo F. Decitabine reverses TGF-β1-induced epithelial–mesenchymal transition in non-small-cell lung cancer by regulating miR-200/ZEB axis. Drug Des, Dev Ther. 2017;11:969–83.
38. Yoshida M, Kijima M, Akita M, Beppu T. Potent and specific inhibition of mammalian histone deacetylase both in vivo and in vitro by trichostatin A. J Biol Chem. 1990;265:17174–9.
39. Knutson SK, Wigle TJ, Warholic NM, Sneeringer CJ, Allain CJ, Klaus CR, et al. A selective inhibitor of EZH2 blocks H3K27 methylation and kills mutant lymphoma cells. Nat Chem Biol. 2012;8:890–6.
40. Meidhof S, Brabletz S, Lehmann W, Preca BT, Mock K, Ruh M, et al. ZEB1-associated drug resistance in cancer cells is reversed by the class I HDAC inhibitor mocetinostat. EMBO Mol Med. 2015;7:831–47.
41. Beckers T, Burkhardt C, Wieland H, Gimmnich P, Ciossek T, Maier T, et al. Distinct pharmacological properties of second generation HDAC inhibitors with the benzamide or hydroxamate head group. Int J Cancer. 2007;121:1138–48.
42. Li R, Liang J, Ni S, Zhou T, Qing X, Li H, et al. A mesenchymal-to-epithelial transition initiates and is required for the nuclear reprogramming of mouse fibroblasts. Cell Stem Cell. 2010;7:51–63.
43. Batlle E, Sancho E, Francí C, Domínguez D, Monfar M, Baulida J, et al. The transcription factor Snail is a repressor of E-cadherin gene expression in epithelial tumour cells. Nat Cell Biol. 2000;2:84–9.
44. Cano A, Pérez-Moreno MA, Rodrigo I, Locascio A, Blanco MJ, del Barrio MG, et al. The transcription factor Snail controls epithelial–mesenchymal transitions by repressing E-cadherin expression. Nat Cell Biol. 2000;2:76–83.
45. Eger A, Aigner K, Sonderegger S, Dampier B, Oehler S, Schreiber M, et al. DeltaEF1 is a transcriptional repressor of E-cadherin and regulates epithelial plasticity in breast cancer cells. Oncogene. 2005;24:2375–85.
46. Aigner K, Dampier B, Descovich L, Mikula M, Sultan A, Schreiber M, et al. The transcription factor ZEB1 (deltaEF1) promotes tumour cell dedifferentiation by repressing master regulators of epithelial polarity. Oncogene. 2007;26:6979–88.
47. Shirakihara T, Saitoh M, Miyazono K. Differential regulation of epithelial and mesenchymal markers by deltaEF1 proteins in epithelial mesenchymal transition induced by TGF-beta. Mol Biol Cell. 2007;18:3533–44.
48. Comijn J, Berx G, Vermassen P, Verschueren K, van Grunsven L, Bruyneel E, et al. The two-handed e box binding zinc finger protein SIP1 downregulates e-cadherin and induces invasion. Mol Cell. 2001;7:1267–78.
49. Vesuna F, van Diest P, Chen JH, Raman V. Twist is a transcriptional repressor of E-cadherin gene expression in breast cancer. Biochem Biophys Res Commun. 2008;367:235–41.
50. Yang J, Mani SA, Donaher JL, Ramaswamy S, Itzykson RA, Come C, et al. Twist, a master regulator of morphogenesis, plays an essential role in tumor metastasis. Cell. 2004;117:927–39.
51. Peng L, Li Y, Xi Y, Li W, Li J, Lv R, et al. MBD3L2 promotes Tet2 enzymatic activity for mediating 5-methylcytosine oxidation. J Cell Sci. 2016;129:1059–71.
52. Minn AJ, Gupta GP, Siegel PM, Bos PD, Shu W, Giri DD, et al. Genes that mediate breast cancer metastasis to lung. Nature. 2005;436:518.
53. Kong D, Ahmad A, Bao B, Li Y, Banerjee S, Sarkar FH. Histone deacetylase inhibitors induce epithelial-to-mesenchymal transition in prostate cancer cells. PLoS ONE. 2012;7:e45045.
54. Jiang G-M, Wang H-S, Zhang F, Zhang K-S, Liu Z-C, Fang R, et al. Histone deacetylase inhibitor induction of epithelial–mesenchymal transitions via up-regulation of Snail facilitates cancer progression. Biochim Biophys Acta (BBA)—Mol Cell Res. 2013;1833:663–71.
55. George JT, Jolly MK, Xu S, Somarelli JA, Levine H. Survival outcomes in cancer patients predicted by a partial EMT gene expression scoring metric. Cancer Res. 2017;77:6415–28.
56. Jolly MK, Boareto M, Huang B, Jia D, Lu M, Ben-Jacob E, et al. Implications of the hybrid epithelial/mesenchymal phenotype in metastasis. Front Oncol. 2015;5:155.
57. Li W, Kang Y. Probing the fifty shades of EMT in metastasis. Trends Cancer. 2016;2:65–7.

58. Aiello NM, Maddipati R, Norgard RJ, Balli D, Li J, Yuan S, et al. EMT subtype influences epithelial plasticity and mode of cell migration. Dev Cell. 2018;45:681–95.e4.
59. Pastushenko I, Brisebarre A, Sifrim A, Fioramonti M, Revenco T, Boumahdi S, et al. Identification of the tumour transition states occurring during EMT. Nature. 2018;556:463–8.
60. Jolly MK, Tripathi SC, Jia D, Mooney SM, Celiktas M, Hanash SM, et al. Stability of the hybrid epithelial/mesenchymal phenotype. Oncotarget. 2016;7:27067–84.
61. Scourzic L, Mouly E, Bernard OA. TET proteins and the control of cytosine demethylation in cancer. Genome Med. 2015;7:9.